All responses will be presented in Times New Roman font. The responses will appear in black, while revisions made to the manuscript will be highlighted in blue.

Reviewer 1

This manuscript examines the role of the OH-initiated H-abstraction pathway in HOM formation from α-pinene photooxidation across a systematic NO range using the SAPHIR-STAR chamber with complementary nitrate-CIMS and propylamine-CIMS. Fuzzy c-means (FCM) clustering is applied to discriminate product families by their temporal formation behavior, and parallel pinonaldehyde photooxidation experiments under matched OH/NO conditions are used to test whether secondary pinonaldehyde oxidation can account for the observed C10H15Ox-related HOM. The study makes a valuable contribution to an unresolved question in monoterpene oxidation chemistry: whether H-abstraction is a negligible curiosity or a substantive contributor to HOM and SOA under NO-rich conditions. The work extends Shen et al. (2022, Sci. Adv.) in three important ways: (i) by systematically varying NO rather than fixing it, (ii) by including a propylamine-CIMS to capture less-oxygenated products (O < 7), and (iii) by providing a direct pinonaldehyde control experiment. The experimental design is sound, the radical budget is well-constrained through a dedicated HO2 calibration via isoprene/MCM modelling, and the conclusions are generally defensible. However, a few comments should be addressed before publication.

Response:

We thank reviewer for his thoughtful review and the positive comments and have addressed all comments in detail below.

Major Comments

1. *Vereecken et al. (2007) suggested that the cleanest diagnostic of H-abstraction is the detection of C10H15Ox species with fewer than five oxygen atoms, since these cannot plausibly arise from OH-addition autoxidation chains. The authors' amine-CIMS data show exactly this: C10H15NO4 is a major peak in ANhigh but is absent from PNhigh (pinal + OH + high NO). Mechanistically, this implies a C10H15O3 peroxy radical precursor, which is the H-abstraction product from α-pinene, and it cannot arise from pinonaldehyde because pinonaldehyde H-abstraction produces C10H15O4 as the nascent RO2. This is the single most compelling piece of evidence in the manuscript and deserves to be highlighted in the abstract, elevated in Section 3.1, and emphasized in the conclusions. At present it is introduced late in Section 3.2 and treated as one observation among many.*

Responses:

We thank the reviewer for this suggestion, which will highlight our convincing evidence for the H-abstraction channel. We have revised the abstract accordingly:

1. ***Revised abstract***

Highly oxygenated organic molecules (HOM) are efficiently formed via autooxidation during ·OH-initiated oxidation of α-pinene. We investigated the relative contributions of ·OH-addition and hydrogen (H)-abstraction to HOM formation from α-pinene photooxidation under varying NO conditions. HOM molecules were detected by a nitrate chemical ionization mass spectrometer (CIMS). In the absence of NO, $C_{10}H_{17}O_x$· peroxy radicals and related termination products (e.g. $C_{10}H_{18}O_x$) dominated the HOM spectrum, accounting for more than 70% of total HOM. The presence of NO substantially altered HOM products, particularly by the rapid formation of $C_{10}H_{15}O_x$·-related HOM like $C_{10}H_{15}NO_8$. The ratio of $C_{10}H_{15}NO_x$ to $C_{10}H_{17}NO_x$ increased significantly from 0.34 to 0.84 as the RO_2· loss rate via reaction with NO increased from 0.18 s^{-1} to 1.06 s^{-1}. Under high-NO conditions, $C_{10}H_{15}O_x$·-related HOM contributed up to 34% to total HOM from α-pinene oxidation systems. H-abstraction channel was proven to be the source of $C_{10}H_{15}O_x$·-related HOM. Fuzzy c-means clustering indicated that $C_{10}H_{15}O_x$·-related HOM exhibited the fastest formation rate among the identified HOM groups, consistent with first-generation products. Comparison with pinonaldehyde oxidation, obtained by normalizing HOM yields to pinonaldehyde turnover, suggests that pinonaldehyde contributed ~5% of HOM in α-pinene systems, excluding secondary oxidation as the dominant source. Detection of $C_{10}H_{15}NO_4$ under high-NO conditions by propylamine-CIMS is indicator for formation of $C_{10}H_{15}O_3$· peroxy radicals, formed by alkoxy radical decomposition and six-membered ring opening in H-abstraction channel. This study highlights the role of the H-abstraction pathway in OH-

initiated α-pinene oxidation under NO-influenced conditions and provides new constraints on detailed HOM formation mechanisms.

We have also revised the conclusions accordingly:

2. Revised Conclusions:

In this study a series of photooxidation experiments was conducted under varying NO levels to investigate the effect of NO on the $C_{10}H_{15}O_x$·-related HOM formation in the α-pinene photooxidation system, and to unravel potential formation pathways of these products. The chemical system was brought to a steady state in the dark. Afterwards, reactions were initiated by photolyzing H_2O_2. We focused on early reaction stages (the first hundreds of seconds), during which RO_2· + NO reactions and RO_2· autoxidation reactions dominate the fate of the RO_2·. $C_{10}H_{17}O_x$·-related HOM are dominantly formed via the ·OH·-addition pathway. Product distributions, potential formation pathways, and rates of $C_{10}H_{17}O_x$·-related HOM have been widely and extensively studied (Berndt, 2021; Xu et al., 2019), and our findings on $C_{10}H_{17}O_x$·-related HOM formation are consistent with previous studies. However, potential formation pathways, distributions, and NO dependence of $C_{10}H_{15}O_x$·-related compounds derived from H-abstraction channel were missing systematic exploration so far.

To constrain the potential contribution of H-abstraction to HOM formation, regimes with and without NO were directly compared, and a separate experiment of pinonaldehyde oxidation under similar conditions was performed. Additionally, measurements by Amine-CIMS were used to detect less oxygenated products. Since the photolysis of H_2O_2 was utilized to produce ·OH radicals O_3 did not accumulate during the early reaction stages; therefore, ozonolysis did not interfere with the ·OH pathways. FCM analysis proves that the dominant species in the $C_{10}H_{15}NO_x$ family, $C_{10}H_{15}NO_8$ and $C_7H_9NO_8$, can be distinguished from other species by their fast formation rates in the presence of NO. Pinonaldehyde oxidation can only contribute ~ 5% to HOM formation in α-pinene oxidation systems. Therefore, neither ozonolysis nor secondary oxidation can explain the significant formation of $C_{10}H_{15}O_x$·-related HOM, which points to H-abstraction from α-pinene by ·OH being the most likely formation pathway.

As illustrated in ***Figure S12*** and ***Figure S16,*** the contribution of the H-abstraction pathway to HOM formation increases with elevated NO levels compared to the ·OH addition pathway. The ratios between major $C_{10}H_{15}O_x$·-related HOM and $C_{10}H_{17}Ox$·-related HOM rise with increasing NO concentrations. The ratios of $C_{10}H_{15}O_x$· peroxy radicals to $C_{10}H_{17}O_x$· peroxy radicals are 0.06, 0.83, and 1.42 under NO-free, low-NO, and high-NO conditions, respectively. Similarly, the ratio of $C_{10}H_{15}NO_x$ to $C_{10}H_{17}NO_x$ increases from 0.34 to 0.84 when NO levels increase from low to high. The sum of major $C_{10}H_{15}O_x$·-related closed-shell HOM products ($C_{10}H_{14}O_x$, $C_{10}H_{15}NO_x$ and $C_{10}H_{16}O_x$) contributes 24% and 34% under low-NO and high-NO conditions, while being negligible under NO-free conditions.

The contribution of H-abstraction related products observed in this study was lower than that reported by Shen and coworkers, who reported a contribution of more than 70% (Shen et al., 2022). The experiments from the two studies were conducted in different chambers, under different conditions and with different instrumentations applied. Two chambers could introduce different wall losses of HOM, which can be further different between less oxygenated HOM and highly oxygenated HOM.

In this study the ·OH radicals were generated via photolysis of H_2O_2, whereas HONO photolysis was the main source of ·OH in Shen et al. (2022). The consecutive reaction between ·OH and H_2O_2 in our experiments leads to an enhanced production of HO_2· radicals, resulting in an HO_2· concentration of ~4 × 10^8 molecule cm^{-3}, which is approximately one order of magnitude higher than that reported by Shen et al. (2022). Also, the NO concentration in Shen et al. was constantly around ~20 ppb, while it was only ~7 ppb before reaction in our study, resulting in a concentration of ~1 ppb during the early-reaction stage. Despite these differences, the contributions of RO_2· + NO reactions are dominant in both studies, accounting for more than 95% of RO_2· biomolecular losses under high-NO conditions. In addition, we did only consider early reaction stages, during which secondary oxidation was negligible and RO_2· chemistry was dominated by autoxidation and RO_2· + NO reactions. Therefore, the chemical system can be expected to be similar for both studies, at least under high-NO conditions. However, the constantly higher level of NO in the study by Shen et al. (2022) may continuously promote the H-abstraction channel.

The discrepancy may also arise from differences in measurement techniques: Shen et al. (2022) used an Eisele type inlet (Mauldin et al., 1999), while in this study a MION inlet was used (Rissanen et al., 2019). To compare both inlet systems, we conducted an experiment where both types of inlets were simultaneously used to measure the same oxidation systems. The reference system was α-pinene oxidation by ·OH, with the addition of NO (***Figure S17).*** The results indicate that the MION inlets detects a larger fraction of lesser oxygenated HOM (less than eight oxygen atoms) than the Eisele inlet, and that these HOM dominate the $C_{10}H_{17}O_x$·-related HOM family, while the relative contribution of higher oxygenated HOM (more than eight oxygen atoms) was larger in the study by Shen et al. (2022). When only the highly oxygenated HOM compounds are considered as was done in the study be Shen and coworkers, the relative contribution of $C_{10}H_{15}O_x$·-related HOM to the total HOM does increase to 64%. Therefore, a deeper comparison of the two inlet types may be of interest in the future but is outside the scope of this study.

These findings indicate that the HOM yield attributed to the H-abstraction pathway compared to the ·OH addition pathway can be significant, and should not be overlooked when assessing the importance of HOM in SOA formation, especially in the presence of NO. Comprehensive product distributions formed through the H-abstraction pathway in α-pinene oxidation are illustrated in this study. HOM species with the formula $C_{10}H_{15}NO_8$, recognized as characteristic indicators of ·OH-initiated monoterpene oxidation in presence of NO under daytime atmospheric conditions (Yan et al., 2016; Kulmala et al., 2013), may potentially be

attributed to the H-abstraction pathway. However, even the NO concentrations in the low-NO case of this study were higher than those typically observed at Hyytiälä. Therefore, the significance of the H-abstraction pathway under typical low-NO boreal forest conditions remains uncertain and requires further investigation. In contrast, the contribution of the H-abstraction channel to HOM formation is expected to be more pronounced in megacities supposed to be under high NO conditions. The presence of NO not only terminates peroxy radicals and suppresses HOM formation, but also propagates the oxidative radical chain through the formation of alkoxy radicals and their subsequent isomerization, a process that under high NO levels can even compete with autoxidation (Kang et al., 2025). These reactions lead to effective NO-NO_2 conversion and can then become a crucial step to promote O_3 formation. The occurrence of alkoxy steps can also directly be related to O_3 formation in addition to O_3 sensitivity via the ratio of organic nitrate and non-nitrate HOM (Zhang et al., 2024). However, branching ratios towards alkoxy radical formation remain uncertain, when RO_2· reacts with NO. Further investigation is needed to clarify the role of alkoxy processes in both SOA and O_3 formation.

2. The authors exclude ozonolysis and pinonaldehyde oxidation (via the FCM timing and the PNhigh control). However, a mechanistic alternative receives little attention: alkoxy radicals derived from C10H17Ox + NO can undergo H-shifts, β-scissions, or HO2 loss steps that might produce 15-H skeletons. This is particularly relevant for the ~75% of four-membered-ring-retained C10H17O3 isomers whose fate under high NO is not extensively discussed here. The authors should (i) explicitly consider whether alkoxy-mediated conversion of C10H17Ox into C10H15Ox products can be quantitatively excluded and (ii) provide an estimate of the contribution this pathway could make given the measured alkoxy branching. The text on lines 262–268 acknowledges alkoxy propagation in the C10H17Ox family but does not connect it to the possibility of subsequent C10H15Ox formation.

Responses:

We thank the reviewer for this comment. However, we can exclude formation of C10H15Ox related alkoxy radicals from the reaction of C10H17Ox with NO for the early experimental stages.

Neither H-migration nor beta-scission in the alkoxy radials will lead to H-loss without breaking the C-C bond, and the resulting alkyl radical will add O2, thus re-starting the C10H17Ox autoxidation chain. $HO_2\cdot$ loss is also unlikely to happen for these molecules as both, H-migration and scission are expected to be favorable (Vereecken and Peeters, 2009, 2010), it takes place it will lead to the formation of a carbonyl and $HO_2\cdot$, resulting in the loss of one H-atom and subsequent formation of C10H16Ox products. While these could in principle react via H-abstraction, leading to C10H15Ox intermediates, this will occur on timescales relevant only for secondary chemistry. For analog reasons it also cannot be an important source for pinonaldehyde. Regarding the contribution of the oxidation of pinonaldehyde to C10H15Ox-derived HOM products, please read our answer to ***Comment 3,*** where we explain in detail why pinonaldehyde oxidation can only contribute up to 10% to the HOM formation in α-pinene oxidation systems.

To clarify this, we extended the related discussion in the manuscript in lines 383-398:

Alkoxy radicals derived from reactions involving $C_{10}H_{17}O_x\cdot$ peroxy radicals and NO can undergo an H-shift, β-scissions, or $HO_2\cdot$ loss steps; however, none of these reactions are expected to form $C_{10}H_{15}O_x\cdot$ peroxy radicals directly. For example, neither H-migration nor β-scission will lead to the loss of a hydrogen atom without a carbon-carbon bond cleavage, and the resulting alkyl radicals will react efficiently with O_2 to regenerate $C_{10}H_{17}O_x\cdot$ radicals and thus continue the autooxidation cycle. The $HO_2\cdot$ loss channel is expected to be a minor pathway for the considered alkoxy radicals, because intramolecular H-migration and β-scission are more favorable, as previously shown by Vereecken and Peeters (Vereecken and Peeters, 2009, 2010). If $HO_2\cdot$ loss channel would happen, it would lead to the formation of carbonyl and $HO_2\cdot$, losing one hydrogen atom forming $C_{10}H_{16}O_x$ products. While the $C_{10}H_{16}O_x$ products could, in principle, react with ·OH radical again to produce $C_{10}H_{15}O_x\cdot$ intermediates, this process would occur on the timescale of

secondary chemistry and is therefore unlikely to contribute significantly during the early reaction stages. Pinonaldehyde was dominant among $C_{10}H_{16}O_x$ compounds, but its oxidation cannot become a significant source of $C_{10}H_{15}O_x$·-related HOM, which will be discussed in Section 3.2.

3. The current argument in Section 3.2 compares summed signals and distributions qualitatively between ANhigh and PNhigh. The authors are suggested to scale the PNhigh yields (per unit pinonaldehyde turnover) by the actual pinonaldehyde concentration and turnover in the ANhigh experiment. Whatever remains must be attributed to primary H-abstraction (or to another non-pinonaldehyde pathway). This arithmetic would transform a qualitative argument into a quantitative upper-bound statement and should be included. Relatedly, the amine-CIMS ratio for C10H15NOx between ANhigh and PNhigh (0.56×) is currently glossed over; because it is less than unity, it seemingly argues for a meaningful pinonaldehyde contribution to the less-oxygenated component, and this deserves an explicit inclusion.

Responses:

We thank the reviewer for this comment. We agree that normalizing major product intensities by the pinonaldehyde turnover of each experiment provides a more appropriate basis for evaluating the contribution of pinonaldehyde oxidation to the formation of C10H15Ox-related HOM observed during α-pinene oxidation.

Previously, we did not calculate the absolute turnover for all the experiments. For the α-pinene oxidation under high-NO conditions and the pinonaldehyde oxidation under high-NO conditions, the turnover ratio was estimated and described as, *'The estimated pinonaldehyde turnover under PN_{high} conditions is ~11 times the turnover as product under AN_{high} conditions.'* Therefore, although the ratio for C10H15NOx between α-pinene case and pinonaldehyde case was ~ 0.56, the pinonaldehyde turnover in pinonaldehyde experiment is much higher than it in α-pinene experiment. Overall, the pinonaldehyde contribution was negligible.

To highlight this evidence and make the comparison between the α-pinene case and the pinonaldehyde case clearer and more convincing, we have made several revisions:

1. We performed model simulations for both the α-pinene-high NO and the pinonaldehyde-high NO experiments to estimate ·OH radical concentrations during the early stages. These simulations were subsequently used to estimate the pinonaldehyde turnover in each experiment, which was shown in Figure 5a (which was previously Figure 4a).
2. We subsequently revised Figure 5b by normalizing the major product intensity by the ratio of the pinonaldehyde turnover obtained from the α-pinene case and the pinonaldehyde case. The updated Figure 5b now shows the average intensities of major products from these two experiments, with the corrected pinonaldehyde turnover.
3. Furthermore, we have expanded the discussion in the manuscript to clarify the normalization procedure and to explicitly account for differences in ·OH exposure and precursor reactivity when

evaluating the role of pinonaldehyde oxidation in the formation of C10H15Ox-related HOM. In summary, we found that the oxidation of pinonaldehyde during the α-pinene oxidation experiments did contribute less than 10% to C10H15Ox-related HOM.

We have updated the figures and text in the manuscript as shown below:

To assess the potential contribution of pinonaldehyde oxidation to the formation of $C_{10}H_{15}O_x$·-related HOM, pinonaldehyde photooxidation experiments were conducted under NO-free and high-NO conditions, analogous to conditions applied in the α-pinene systems (***Table 1***). Time series of α-pinene and its oxidation product pinonaldehyde during the first 30 min of the α-pinene (high-NO) experiment are shown in Figure ***5(a-1).*** The corresponding turnovers of α-pinene and pinonaldehyde are presented in Figure ***5(a-1).*** Similarly, the concentration of pinonaldehyde and its turnover during the pinonaldehyde (high-NO) experiment are shown in Figure ***5(a-2).*** ·OH concentrations were estimated using model simulations.

During early stage, the average pinonaldehyde turnover was 8.9×10^6 molecules cm^{-3} s^{-1} under pinonaldehyde (high-NO) condition, approximately 6 times higher than the turnover (1.5×10^6 molecules cm^{-3} s^{-1}) under α-pinene (high-NO) condition. To facilitate comparison between the two experiments, we calculated the pinonaldehyde turnover for both experiments and compared it to obtain the ratio between the high-NO α-pinene and pinonaldehyde experiment (hereafter referred to as the pinonaldehyde turnover ratio). Signals measured in the pinonaldehyde experiment were subsequently normalized by this ratio to account for differences in the pinonaldehyde turnover between the two experimental systems. The distributions of major $C_{10}H_{15}O_x$·-related products observed during the high-NO α-pinene and high-NO pinonaldehyde experiments are presented in Figure 5(b). Major products belonging to the $C_{10}H_{14}O_x$ and $C_{10}H_{15}NO_x$ family detected by both nitrate-CIMS (N) and amine-CIMS (A) are included. The data shown in ***Figure 5(b)*** represents averages over the first 320 s following the initiation of oxidation, corresponding to the early reaction stage, during which RO_2· + NO accounts for more than 90% of the total bimolecular RO_2· loss rate. In addition, all product signals here as well as all data used for comparison in the following paragraphs have been normalized by the pinonaldehyde turnover.

The pinonaldehyde turnover ratio during the first 320 s exceeded 5 and was substantially higher during the first 100 s. This large difference arises because pinonaldehyde was present at the start of the pinonaldehyde high-NO experiment and was therefore immediately available for reaction with ·OH. In contrast, under α-pinene high-NO conditions, pinonaldehyde had to be formed through α-pinene oxidation before it could undergo further reactions, resulting in a much lower pinonaldehyde turnover during the early stages of the experiment. For $C_{10}H_{15}O_x$·-related HOM detected by nitrate-CIMS the summed signals of the $C_{10}H_{14}O_x$ and $C_{10}H_{15}NO_x$ families under α-pinene high-NO conditions exceed those of pinonaldehyde high-NO conditions by factors of approximately 20 and 10, respectively. Although pinonaldehyde oxidation contributes to the formation of $C_{10}H_{15}O_x$·-related HOM under high-NO conditions, this contribution is

minor and can explain approximately 5% of the HOM yield observed from α-pinene oxidation. Similarly, for less oxygenated products measured by amine-CIMS, the summed concentrations of the $C_{10}H_{14}O_x$ and $C_{10}H_{15}NO_x$ families were 98 times higher in the α-pinene high-NO experiment, and 6.7 times higher in the pinonaldehyde high-NO experiment.

For highly oxygenated compounds detected by nitrate-CIMS, species containing more than 10 oxygen atoms account for 11% of the $C_{10}H_{14}O_x$ family and for 13% of the $C_{10}H_{15}NO_x$ family under α-pinene high-NO condition, whereas their contributions are much lower for pinonaldehyde high-NO conditions (3% and 5%, respectively).

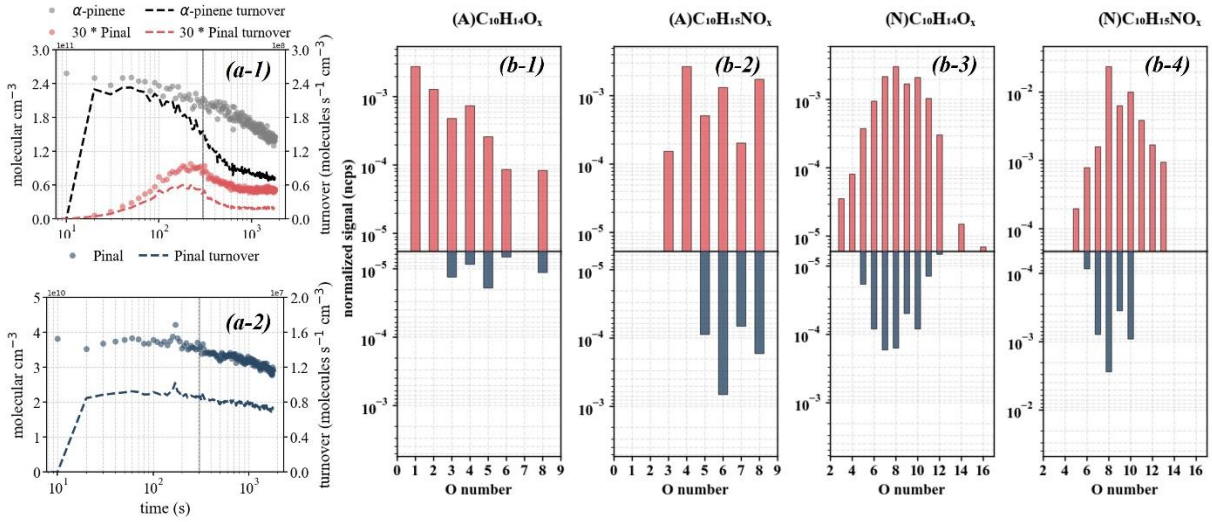

Figure 5. Panel (a-1) displays concentrations and turnover of α-pinene and pinonaldehyde (Pinal) during α-pinene photooxidation under high-NO conditions, while panel (a-2) represents concentrations and turnover of pinonaldehyde during the high-NO pinonaldehyde photooxidation experiment. Major product distributions are shown in panel (b-1) to (b-4). Signals detected in the pinonaldehyde experiment are normalized by the ratio of the pinonaldehyde turnover during the pinonaldehyde experiment to the respective turnover during the α-pinene experiment. The products are separated into four groups: (A)$C_{10}H_{14}O_x$, (A)$C_{10}H_{15}NO_x$, (N)$C_{10}H_{14}O_x$, (N)$C_{10}H_{15}NO_x$, of which (A) and (N) represent signals derived from amine-CIMS and nitrate-CIMS, respectively. Data from α-pinene oxidation and pinonaldehyde oxidation are colored in pink and blue, respectively.

4. The inference of generation order from cluster peak times (160, 210, 290, 850 s for clusters 1–4) is central to the argument that C10H15NO7/NO8 are first-generation products and that pinonaldehyde (in cluster 3) cannot be their precursor. Several uncertainties are not addressed: (1) The four-cluster solution was selected from SSE, distortion, and silhouette curves (Figure S5), but robustness of the cluster-1 membership of C10H15NO7/NO9 under 3- and 5-cluster solutions should be tested. (2) Early-peaking behavior does not strictly imply first-generation status; species formed rapidly from short-lived precursors can also peak early. (3) The FCM run of 50 initializations per cluster number presumably yields a distribution of cluster assignments; the authors should report how stable cluster-1 membership is across these initializations.

Responses:

We thank the reviewer for the comments and suggestions. We have extensively tested the clustering with several possible cluster solutions and varying parameters to check the stability of clustering results, analog to the procedure previously developed and described in (Wu et al., 2024). We will discuss the previously obtained results from the 3- and 5-cluster solutions here and have also included them in the manuscript and the supplemental material, as suggested by the reviewer.

When investigating 3- and 5-cluster solutions we found that the conclusions from the manuscript remain, meaning that the HOM indicators derived from the H-abstraction channel (e.g., C10H15NO8 and C7H9NO8) were always attributed to the first emerging cluster. The results of 3-cluster solution and 5-cluster solution are shown below.

Regarding (2): in our manuscript (analog to definitions often used in atmospheric chemistry), first-generation products are defined as closed-shell species formed directly from the initial oxidation of the precursor, without subsequent oxidation steps. In this framework, the temporal evolution of a compound is determined by both its formation and loss processes. For HOM we consider wall-loss as the dominant sink for our experimental conditions. While wall-loss rates may vary to some extent among compounds, such differences are expected to be smaller than the variability in formation rates under the same conditions. Therefore, the observed differences in time profiles are primarily interpreted as reflecting differences in formation rates. Under this assumption, compounds exhibiting earlier signal maxima are associated with faster formation and thus more likely represent first-generation products.

To test the stability of the clustering results, as suggested in (3), we ran the clustering 50 times with different initializations for the four-cluster solution, and investigated the cluster assignment for all key compounds, such as $C_{10}H_{15}NO_8(NO_3^-)$, $C_7H_9NO_8(NO_3^-)$ and $C_{10}H_{16}O_2(C_3H_7NH_3^+)$. The results demonstrated a very high clustering stability, as these compounds were consistently assigned to the same

cluster across all runs. For example, $C_{10}H_{15}NO_8(NO_3^-)$ was assigned to the first cluster in all clustering runs. Therefore, the clustering results and insights derived from them are highly robust and reliable.

Below we attached the text and figures which were added to the manuscript and the supplement. Revised or added text is shown in blue.

To assess the robustness of the clustering results, additional cluster analysis was performed using a three- and five-cluster solution, as shown in ***Figure S13*** and ***Figure S14***, respectively. Consistent conclusions are obtained regardless of the number of clusters specified. In particular, the key compounds derived from the H-abstraction channel, such as $C_{10}H_{15}NO_8(NO_3^-)$ and $C_7H_9NO_8(NO_3^-)$, were consistently assigned to the first cluster with the fastest formation rate. The stability of the clustering results was further evaluated by performing 50 clustering runs with random initializations and using the four-cluster solution. The distributions of the cluster assignments were then analyzed, as shown in ***Figure S15***, with particular attention given to the key compounds discussed above, including $C_{10}H_{15}NO_8(NO_3^-)$, $C_7H_9NO_8(NO_3^-)$, and $C_{10}H_{16}O_2(C_3H_7NH_3^+)$. The results demonstrate the high stability of the cluster solution, as these compounds were consistently assigned to the same cluster across all runs. For example, $C_{10}H_{15}NO_8(NO_3^-)$ was assigned to the first cluster in all runs. Therefore, the clustering results and insights derived from them are highly robust and reliable.

The compounds $C_{10}H_{15}NO_7(NO_3^-)$ and $C_{10}H_{15}NO_8(NO_3^-)$ are assigned to cluster 1 with the fastest formation rate; thus, they are likely first-generation products.

Changes added to the supplemental information:

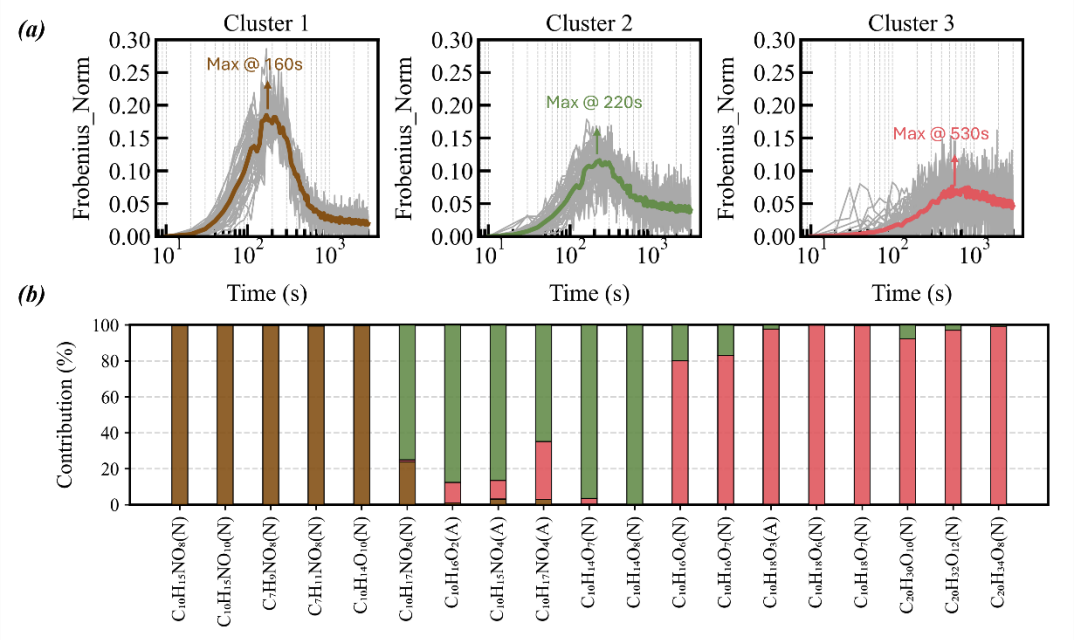

Figure S13. Results of fuzzy c-means clustering for three clusters for the dominant signals (156 in total) during early reaction stages of α-pinene photooxidation under high-NO condition are shown in panel ***(a)***.

The time series of the cluster centers are displayed as colored solid lines, while individual contributing species are shown as gray lines. Panel ***(b)*** illustrates the cluster apportionment of selected major products detected in both nitrate-CIMS (N) and amine-CIMS (A).

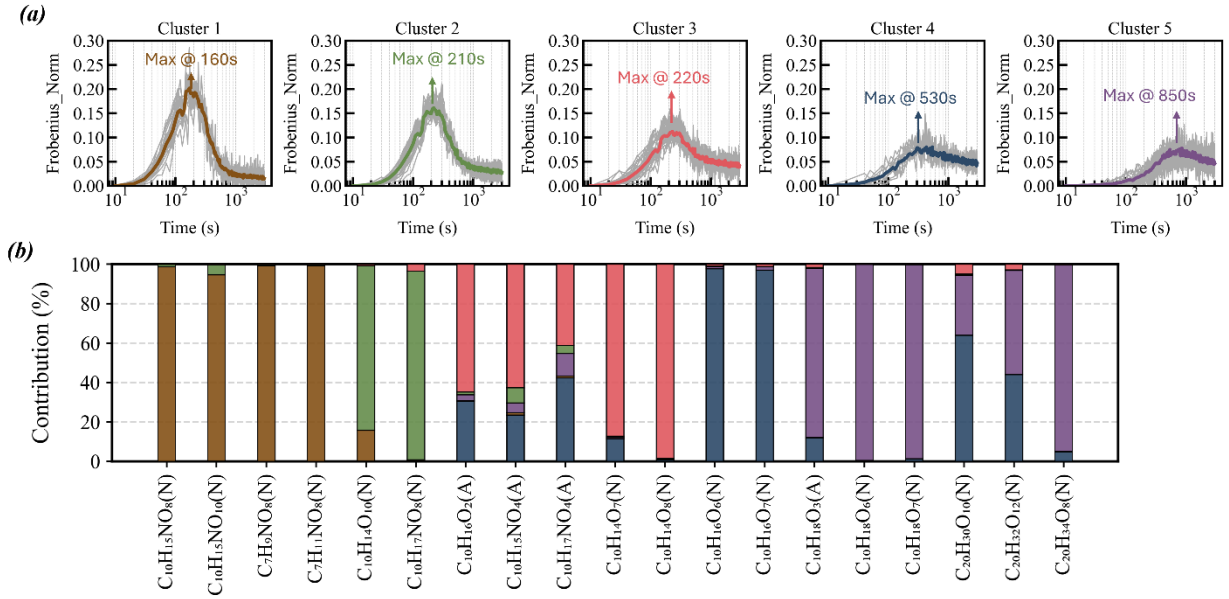

Figure S14. Results of fuzzy c-means clustering for five clusters for the dominant signals (156 in total) during early reaction stages of α-pinene photooxidation under high-NO condition are shown in panel ***(a)***. The time series of the cluster centers are displayed as colored solid lines, while individual species are shown as gray lines. Panel ***(b)*** illustrates the cluster apportionment of selected major products detected in both nitrate-CIMS (N) and amine-CIMS (A).

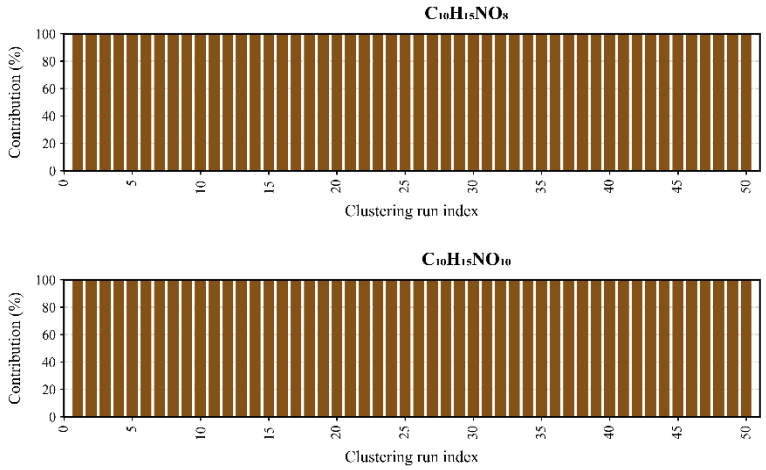

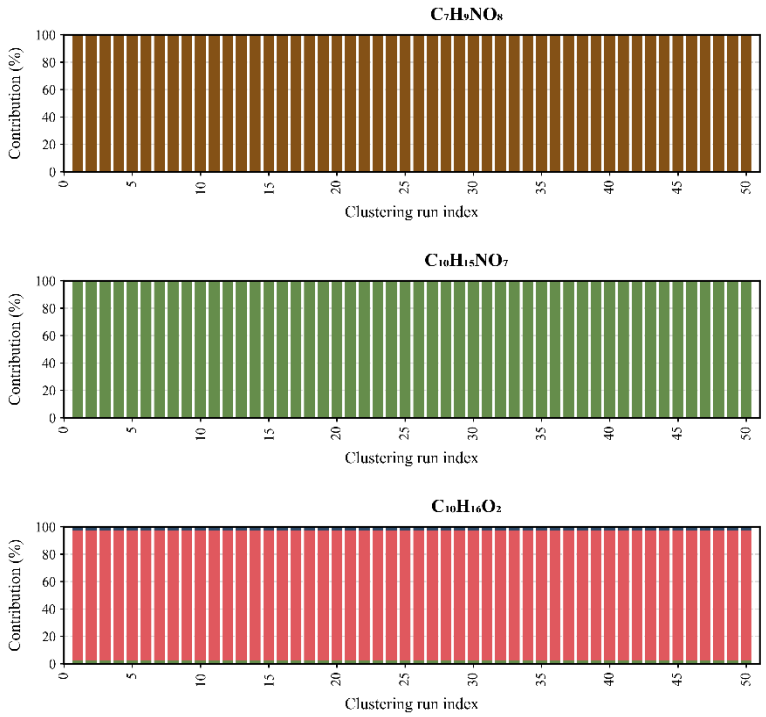

Figure S15. The results of 50 independent clustering runs using a four-cluster solution and random initialization are shown. The distributions of cluster assignments for key compounds are evaluated, including $C_{10}H_{15}NO_8(NO_3^-)$, $C_{10}H_{15}NO_{10}(NO_3^-)$, $C_7H_9NO_8(NO_3^-)$, $C_{10}H_{15}NO_7(NO_3^-)$, and $C_{10}H_{16}O_2(C_3H_7NH_3^+)$.

5. The H-abstraction contribution reported here (~30% of HOM under ANhigh) is described as "70% lower than" Shen et al. The proposed explanation (Eisele inlet vs. MION inlet detection efficiency for less-oxygenated C10H17Ox-related HOM) is highly speculative. The two studies also differ in chamber, residence time, NO range, VOC concentration, and OH source. A more detailed discussion would be helpful.

Responses:

We thank the reviewer for this insightful comment. We agree that the comparison with Shen et al. should be interpreted with more caution, as the two studies were conducted under different experimental conditions. In the revised manuscript, we have expanded the discussion and now explicitly address several factors that may contribute to the discrepancy, including differences in reaction time, RO2 fates under high-NO conditions, and instrumental setup.

Although we performed experiments with different ·OH sources, the level of and exposure to ·OH are comparable between the two experiments. In the experiments presented in the manuscript, more HO_2· radicals were produced due to the reaction between H_2O_2 and OH, resulting in HO_2· concentrations which were around one order of magnitude higher than those in Shen et al.'s study. However, box model simulations we performed show that under high-NO conditions the RO_2· + NO reaction rate can explain more than 95% of bimolecular RO_2· losses, which is consistent with Shen et al. Since only early-reaction stages were considered for both studies, during which secondary oxidation is negligible, and RO_2· + NO dominate RO_2· biomolecular reactions, the chemical regimes of both studies are very similar and comparable. The different chamber setups have different wall loss rates, which can lead to larger uncertainties for determining and comparing HOM yields and product distributions.

Regarding the proposed explanation related to the inlet systems, we agree that the interpretation was insufficiently described and supported in the previous version of our manuscript. To strengthen this discussion, we now include evidence from previous intercomparisons and measurements that were specifically designed to evaluate the performance of an Eisele and a MION inlet system. The measurements suggest that the detection efficiency for less-oxygenated HOM (O<8) differs between the two inlet configurations. For example, less-oxygenated C10H17Ox-related HOM were detected with higher efficiency by the MION inlet (***Figure S17***). Therefore, the relative contribution of C10H15Ox-related HOM might be higher in the Eisele inlet. Since this study used a MION inlet, whereas Shen et al. used an Eisele inlet, inlet-dependent sensitivity differences could partly explain the lower contribution of H-abstraction-related products observed in this study.

We extended the discussion and added one more plot to show the different measurement results between the Eisele and the MION inlet (Figure S17):

The contribution of H-abstraction related products observed in this study was lower than that reported by Shen and coworkers, who reported a contribution of more than 70% (Shen et al., 2022). The experiments from the two studies were conducted in different chambers, under different conditions and with different instrumentations applied. Two chambers could introduce different wall losses of HOM, which can be further different between less oxygenated HOM and highly oxygenated HOM.

In this study the ·OH radicals were generated via photolysis of H_2O_2, whereas HONO photolysis was the main source of ·OH in Shen et al. (2022). The consecutive reaction between ·OH and H_2O_2 in our experiments leads to an enhanced production of HO_2· radicals, resulting in an HO_2· concentration of ~4×10^8 molecule cm^{-3}, which is approximately one order of magnitude higher than that reported by Shen et al. (2022). Also, the NO concentration in Shen et al. was constantly around ~20 ppb, while it was only ~7 ppb before reaction in our study, resulting in a concentration of ~1 ppb during the early-reaction stage. Despite these differences, the contributions of RO_2· + NO reactions are dominant in both studies, accounting for more than 95% of RO_2· biomolecular losses under high-NO conditions. In addition, we did only consider early reaction stages, during which secondary oxidation was negligible and RO_2· chemistry was dominated by autoxidation and RO_2· + NO reactions. Therefore, the chemical system can be expected to be similar for both studies, at least under high-NO conditions. However, the constantly higher level of NO in the study by Shen et al. (2022) may continuously promote the H-abstraction channel.

The discrepancy may also arise from differences in measurement techniques: Shen et al. (2022) used an Eisele type inlet (Mauldin et al., 1999), while in this study a MION inlet was used (Rissanen et al., 2019). To compare both inlet systems, we conducted an experiment where both types of inlets were simultaneously used to measure the same oxidation systems. The reference system was α-pinene oxidation by ·OH, with the addition of NO (***Figure S17).*** The results indicate that the MION inlets detects a larger fraction of lesser oxygenated HOM (less than eight oxygen atoms) than the Eisele inlet, and that these HOM dominate the $C_{10}H_{17}O_x$·-related HOM family, while the relative contribution of higher oxygenated HOM (more than eight oxygen atoms) was larger in the study by Shen et al. (2022). When only the highly oxygenated HOM compounds are considered as was done in the study be Shen and coworkers, the relative contribution of $C_{10}H_{15}O_x$·-related HOM to the total HOM does increase to 64%. Therefore, a deeper comparison of the two inlet types may be of interest in the future but is outside the scope of this study.

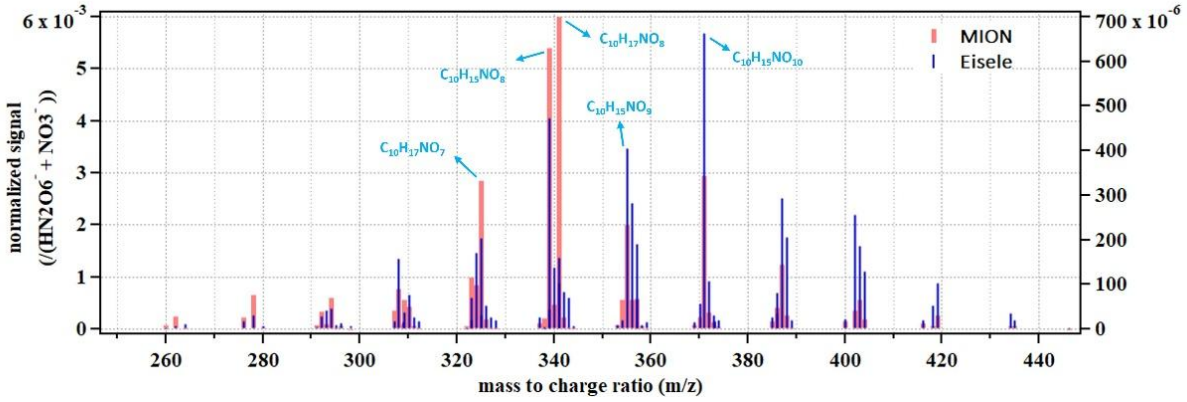

Figure S17. The signal of products derived from α-pinene oxidation with NO injection, detected by CIMS coupled with the MION (pink) and Eisele (blue) inlets.

6. HO2 varies by a factor of ~3 across conditions. Because $HO_2\cdot$ is a competing sink for both C10H17Ox and C10H15Ox and because the C10H16Ox family assignment explicitly invokes C10H15Ox + HO2, the varying HO2 should be more prominently incorporated into the interpretation of C10H15Ox-related HOM yields. It would be useful to present yields normalized by the relevant rate-weighted sink flux rather than by raw VOC turnover.

Responses:

We thank the reviewer for this comment. We agree that $RO_2\cdot + HO_2\cdot$ reactions are an important termination pathway for $RO_2\cdot$ radicals and can influence the product distribution and thereby potentially the yields of C10H15Ox-related HOM. For the C10 monomer HOM investigated here, both C10H14Ox and C10H15NOx are expected to originate from C10H15Ox radicals. We have shown above that the H-abstraction pathway is the dominant source of these C10H15Ox radicals.

In addition, some compounds within the C10H16Ox group may also be formed through termination reactions of C10H15Ox radicals, for example via C10H15Ox + $HO_2\cdot$ → C10H16Ox or C10H15Ox + $RO_2\cdot$ → C10H16Ox (-OH). Compounds assigned to the C10H16Ox group can also be produced from C10H17Ox radicals through termination reactions such as C10H17Ox + $RO_2\cdot$ → C10H16Ox (=O). Therefore, it is difficult to unambiguously distinguish whether a given C10H16Ox compound originates from C10H15Ox or C10H17Ox radicals solely based on our measurements. Consequently, a quantitative separation of the C10H16Ox group into products derived from these two radical pathways would come with high uncertainties.

Like the formation pathways of C10H16Ox, which involves C10H15Ox, C10H18Ox can also be produced when C10H17Ox reacts with $RO_2\cdot$ and $HO_2\cdot$ radicals. If we assume similar bimolecular reaction rate constants for C10H15Ox and for C10H17Ox with NO, $HO_2\cdot$, and $RO_2\cdot$, and further that the $RO_2\cdot$ fate is the same for these product classes under comparable conditions, then the loss pathways of C10H15Ox and C10H17Ox can be also considered similar. Under these assumptions, the ratio of C10H18Ox to C10H17NOx can be approximated as equivalent to the ratio of C10H16Ox (derived from C10H15Ox) to C10H15NOx. This relationship may provide a potential approach to estimate the partitioning of C10H16Ox compounds into two groups.

Therefore, to elucidate the contribution of H-abstraction to HOM yields under varying $RO_2\cdot$ fates, we performed box model simulations to estimate the radical concentrations during the early reaction stages, and then tried to quantitively estimate the relative contributions of the different biomolecular reactions of $RO_2\cdot + HO_2\cdot$, $RO_2\cdot + RO_2\cdot$, and $RO_2\cdot$ + NO to the total biomolecular losses for all $RO_2\cdot$. Based on the results from the simulations and estimates, contributions of C10H15Ox-related HOM are negligible for conditions without NO while contributing ~24% and ~34%, for low-NO and high-NO conditions, respectively.

To emphasize and clarify these conclusions we added descriptions about the model simulations and the definitions of early reaction stages to the manuscript. Additionally, the conclusions about the contributions of C10H15Ox-related HOM were revised accordingly.

The updated figures and text to determine RO_2· fates under different conditions are attached below:

Model simulations to determine early reaction stages

To clarify the role of the H-abstraction channel under varying NO conditions the early reaction stages are particularly relevant. In this study, we define early reaction stages using three criteria: (i) α-pinene turnover exceeds that of pinonaldehyde by a factor of ten, (ii) under conditions with NO, biomolecular reactions of RO_2· are dominated by RO_2· + NO and contribute more than 90% to the biomolecular loss of RO_2·, and (iii) α-pinene oxidation is primarily driven by OH· rather than O_3. Therefore, model simulations for α-pinene photooxidation systems were conducted to quantitively identify these early reaction stages.

As shown in ***Figure 2 (a-1) to (c-1)***, the model captures the evolution of the system quite well but generally underestimates NO and O_3 concentrations. These discrepancies may arise from differences in the temporal resolution of measurements and simulations, physical effects introduced by the activation of the UVC lamps (e.g., changing emissions due to temperature adjustment of the UVC lamp), and uncertainties in the chemical mechanism including reactions currently not represented in the model framework. The HO_2· and RO_2· concentrations obtained from the simulations are shown in ***Figure 2 (a-2) to (c-2)*** together with the relative contributions of RO_2· + NO, RO_2· + HO_2· and RO_2· + NO to the total biomolecular RO_2 loss. Here, the reaction rates were calculated with $k_{[RO2][HO2]} = 1.85 \cdot 10^{-11}$ cm^3 s^{-1}, $k_{[RO2][NO]} = 1 \cdot 10^{-11}$ cm^3 s^{-1} and $k_{[RO2][RO2]} = 5 \cdot 10^{-12}$ cm^3 s^{-1} (Baker et al., 2024; Berndt et al., 2016; Jenkin et al., 1997).

Based on these results, reactions occurring within the first 100 s, 100 s, and 320 s after initiation of reactions by starting the photooxidation were defined as early stages for the NO-free, low-NO, and high-NO conditions, respectively. The average bimolecular reaction rates for RO_2· + NO were negligible for cases without NO and increased to 0.179 s^{-1} and 1.06 s^{-1} for the low-NO and high-NO conditions, respectively. For RO_2· + HO_2· reactions, the rates were 0.0055 s^{-1}, 0.011 s^{-1}, and 0.0075 s^{-1}, while those for RO_2· + RO_2· reactions were 0.0075 s^{-1}, 0.0029 s^{-1}, and 0.0014 s^{-1} for NO-free, low-NO, and high-NO conditions, respectively. The contribution of RO_2· + NO was higher than 90% under both low-NO and high-NO conditions.

For pinonaldehyde photooxidation under high-NO conditions, the reactions within the early reaction stages were also investigated to facilitate comparison with the corresponding α-pinene system under high NO conditions. Besides H-abstraction channel, reactions of α-pinene with O_3, and pinonaldehyde with ·OH may also contribute to the formation of $C_{10}H_{15}O_x$ radicals. Therefore, the loss of α-pinene due to oxidation by O_3 formed as a byproduct of other reactions, and the loss of pinonaldehyde via OH oxidation, were evaluated. The results are shown in detail in ***Figure S7***. In both cases, losses are smaller than 1% of the

reaction rate of α-pinene with OH·, which further supports our definition of early reaction stage being reasonable and representative.

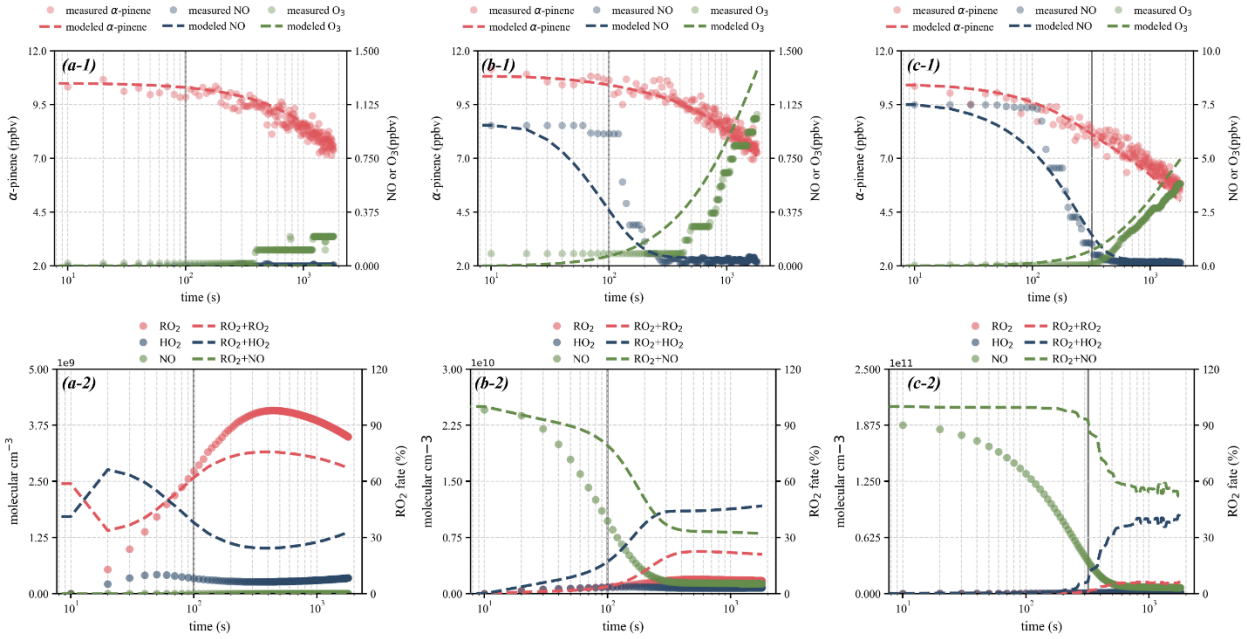

Figure 2. Results of model simulations for α-pinene photooxidation under NO-free (a-1, a-2), low-NO (b-1, b-2), and high-NO conditions (c-1, c-2). The upper panels show modeled and measured concentrations of α-pinene, NO, and O_3 across the three conditions, while the lower panels show the corresponding radical concentrations of RO_2· and HO_2·. In addition, the lower panels illustrate the relative contributions of RO_2· + HO_2·, RO_2· + RO_2· and RO_2· + NO reactions to the total bimolecular reaction rate of RO_2· (shown as RO_2· fate on the right y-axis).

We also updated the conclusions accordingly:

The sum of the major $C_{10}H_{15}O_x$·-related closed-shell HOM products ($C_{10}H_{14}O_x$, $C_{10}H_{15}NO_x$ and $C_{10}H_{16}O_x$) contributes 24% and 34% to the total HOM under low-NO and high-NO conditions, while it is negligible under NO-free conditions.

7. The extrapolation to Hyytiälä and to megacity conditions should be more carefully framed. Hyytiälä daytime NO is typically well below 0.5 ppbv, whereas the dominant H-abstraction signal here is observed at 7.4 ppbv. A quantitative statement of how the H-abstraction HOM fraction scales between the lab ranges explored and atmospherically relevant NO levels would be valuable and would temper the implied relevance to low-NO boreal conditions.

Responses:

We thank reviewer for this comment and the suggestion. We agree that direct extrapolation from our chamber conditions to Hyytiälä requires careful consideration and quantitative evaluation. Therefore, in the updated manuscript, we have made several modifications.

1. We performed box model simulations to quantitively estimate $RO_2\cdot$ fates under different experimental conditions, especially regarding the different NO conditions used. Please find the details in our responses to ***Comment 6***.
2. A more detailed comparison between this study and Shen et al. (2022) was extended, which was addressed in our responses to ***Comment 5***.
3. The contribution of H-abstraction to the total HOM formation is now discussed for both high-NO and low-NO conditions, and the corresponding statements in the Abstract and the Conclusions have been revised accordingly, which can be found in our responses to ***Comment 1***.

The application of results observed in our chamber study to the field case (Hyytiälä) was revised accordingly to account for possible uncertainties. The revised part of the Conclusion can be found ***in Comment 1.***

References:

Baker, Y., Kang, S., Wang, H., Wu, R., Xu, J., Zanders, A., He, Q., Hohaus, T., Ziehm, T., Geretti, V., Bannan, T. J., O'Meara, S. P., Voliotis, A., Hallquist, M., McFiggans, G., Zorn, S. R., Wahner, A., and Mentel, T. F.: Impact of HO2⁄RO2 ratio on highly oxygenated α-pinene photooxidation products and secondary organic aerosol formation potential, Atmos. Chem. Phys., 24, 4789-4807, 10.5194/acp-24-4789-2024, 2024.

Berndt, T., Richters, S., Jokinen, T., Hyttinen, N., Kurten, T., Otkjaer, R. V., Kjaergaard, H. G., Stratmann, F., Herrmann, H., Sipila, M., Kulmala, M., and Ehn, M.: Hydroxyl radical-induced formation of highly oxidized organic compounds, NATURE COMMUNICATIONS, 7, 10.1038/ncomms13677, 2016.

Berndt, T.: Peroxy Radical Processes and Product Formation in the OH Radical-Initiated Oxidation of alpha-Pinene for Near-Atmospheric Conditions, J Phys Chem A, 125, 9151-9160, 10.1021/acs.jpca.1c05576, 2021.

Jenkin, M. E., Saunders, S. M., and Pilling, M. J.: The tropospheric degradation of volatile organic compounds: a protocol for mechanism development, Atmospheric Environment, 31, 81-104, https://doi.org/10.1016/S1352-2310(96)00105-7, 1997.

Kang, S., Wildt, J., Pullinen, I., Vereecken, L., Wu, C., Wahner, A., Zorn, S. R., and Mentel, T. F.: Formation of highly oxygenated organic molecules from α-pinene photooxidation: evidence for the importance of highly oxygenated alkoxy radicals, EGUsphere, 2025, 1-33, 10.5194/egusphere-2025-2772, 2025.

Kulmala, M., Kontkanen, J., Junninen, H., Lehtipalo, K., Manninen, H. E., Nieminen, T., Petäjä, T., Sipilä, M., Schobesberger, S., Rantala, P., Franchin, A., Jokinen, T., Järvinen, E., Äijälä, M., Kangasluoma, J., Hakala, J., Aalto, P. P., Paasonen, P., Mikkilä, J., Vanhanen, J., Aalto, J., Hakola, H., Makkonen, U., Ruuskanen, T., Mauldin, R. L., Duplissy, J., Vehkamäki, H., Bäck, J., Kortelainen, A., Riipinen, I., Kurtén, T., Johnston, M. V., Smith, J. N., Ehn, M., Mentel, T. F., Lehtinen, K. E. J., Laaksonen, A., Kerminen, V.-M., and Worsnop, D. R.: Direct Observations of Atmospheric Aerosol Nucleation, Science, 339, 943-946, 10.1126/science.1227385, 2013.

Mauldin, R. L., Tanner, D. J., Heath, J. A., Huebert, B. J., and Eisele, F. L.: Observations of H2SO4and MSA during PEM-Tropics-A, Journal of Geophysical Research: Atmospheres, 104, 5801-5816, 10.1029/98jd02612, 1999.

Shen, H., Vereecken, L., Kang, S., Pullinen, I., Fuchs, H., Zhao, D., and Mentel, T. F.: Unexpected significance of a minor reaction pathway in daytime formation of biogenic highly oxygenated organic compounds, Science Advances, 8, eabp8702, doi:10.1126/sciadv.abp8702, 2022.

Xu, L., Moller, K. H., Crounse, J. D., Otkjaer, R. V., Kjaergaard, H. G., and Wennberg, P. O.: Unimolecular Reactions of Peroxy Radicals Formed in the Oxidation of alpha-Pinene and beta-Pinene by Hydroxyl Radicals, J Phys Chem A, 123, 1661-1674, 10.1021/acs.jpca.8b11726, 2019.